Revisiting the Effects of the Molecular Structure in the Kinetics of Electron transfer of Quinones: Kinetic Differences in Structural Isomers

Carlos Frontana[1*] and Ignacio González[2]

[1] Centro de Investigación y de Estudios Avanzados del Instituto Politécnico Nacional Departamento de Química, Av. Instituto Politécnico Nacional No. 2508. Col. San Pedro Zacatenco, C. P. 07360. México, DF., México, Tel. 52-55-50613800 Ext. 4001, Fax. 52-55-50613389. e-mail: ultrabuho@yahoo.com.mx

[2] UAM-Iztapalapa, Depto. de Química, Área de Electroquímica, Apartado postal 55-534, 09340, México, D.F.

Abstract. The effect of 2,5 and 2,6 disubstitution (R = CH_3, Cl, $C(CH_3)_3$) for 1,4-benzoquinones, in the reorganization energy (λ) for the first electron uptake process was analyzed in acetonitrile solution. Data obtained by cyclic voltammetry suggested differences in λ for each type of disubstitution analyzed. These differences have important consequences in the stability and structure of the electrogenerated benzosemiquinone species, which was verified by performing *in-situ* spectroelectrochemical-ESR (Electron Spin Resonance) experiments of each disubstituted semiquinone.
Key words: Quinone, substituent effect, cyclic voltammetry, inner reorganization energy, ESR

Resumen. El efecto de la disustitución 2,5 y 2,6 (R = CH_3, Cl, $C(CH_3)_3$) para diferentes 1,4-benzoquinonas, en la energía de reorganización (λ) para el primer proceso de reducción analizado en acetonitrilo. Los datos obtenidos por voltamperometría cíclica sugieren diferencias en λ entre cada tipo de disustitución analizada. Estas diferencias tienen consecuencias importantes en la estabilidad y estructura de las especies benzo-semiquinona electrogeneradas, lo que fue evidenciado en el análisis *in situ* espectroelectroquímico-ESR (Resonancia del Espín Electrónico) de cada semiquinona disustituida.
Palabras clave: Quinona, efecto de sustituyente, voltamperometría cíclica, energía de reorganización interna, ESR

Introduction

Quinones represent a biologically reactive group of molecules, presenting a high citotoxicity [1]. This reactivity, among other factors, is due to the ability that the quinone group has to undergo electron transfer processes related to the generation of Reactive Oxygen Species (ROS, e.g. superoxide anion radical and H_2O_2) in biological systems [2, 3]. As in these processes a reactive radical species is generated (semiquinone), the biological activity of a given quinone compound is determined by the stability of this intermediate. In such terms, electrochemical experiments can be helpful to analyze the stability and energetics on the formation of semiquinones. For this purpose, the use of aprotic media or aqueous basic conditions is advantageous, as this type of intermediates can be stabilized and studied properly [4, 5, 6].

An alternative to study this type of compounds is to analyze the substituent effect in the energetics of heterogeneous electron transfer, employing the Hammett formalism [7, 8]. However, even when this approach appears to be quite simple it should be remarked that, during the electron transfer process, the chemical characteristics of not only the reactant species are important, but also on the product of the reduction [9]. Therefore, a complete description of how the substituent affects the electron transfer pathway depends on the chemical properties of both species participating.

The approach in terms of the Marcus-Hush theory appears more useful, as this theory deals on how do the chemical properties of both reduced and oxidized species affect the electron transfer kinetics [10, 11, 12, 13]. The most important feature of this theory is the proposal that the Gibbs free energy of activation during the electron transfer process ($\Delta G^\ddagger$), is dependent on a parameter (λ) which accounts on the effects of the structural reorganization processes occurring during the electron transfer, as follows

$$\Delta G^\ddagger = \frac{\lambda}{4}\left(1 + \frac{F(E - E^0)}{\lambda}\right)^2. \qquad (1)$$

This parameter -the reorganization energy (λ)-, represents the energy needed to transform the nuclear configurations in the reactant and the solvent to the product state [**14**]. At E^0, $\Delta G^\ddagger$ is equal to $\lambda/4$ [**14**] and therefore is possible to estimate it from electrochemical experiments, as the apparent rate constant of electron transfer (k_s), becomes:

$$k_s = A\exp(-\Delta G^\ddagger / RT). \qquad (2)$$

Furthermore, the electrochemical transfer coefficient – α -, also has a dependency on λ following the expression:

$$\alpha = \frac{1}{2} + \frac{F(E - E^0)}{2\lambda}. \qquad (3)$$

Two contributions are proposed that account for the total reorganization energy: λ_i (inner) and λ_o (outer) reorganization energies:

$$\lambda = \lambda_i + \lambda_o,$$

λ_i represents the contribution of the reorganization of the bond angles and distances in the reduced (or oxidized) species during the electron transfer. λ_o represents the energy needed to reorganize the solvation sphere during the electron uptake, associated to the size of the molecule.

In the case of the study of electron transfer kinetics in quinones, most of the work previously informed account for more important changes in the outer reorganization term [15, 16]. In the work of Clegg and coworkers [16], the inner reorganization term is completely neglected. As electronic effects are decisive in the stabilization of the reduced form of the quinone (semiquinone), they should affect the inner reorganization term, so it is required a more detailed study on this matter. An interesting case for studying experimentally such effects would be the one dealing with structural isomers (e. g. 2,5 and 2,6 disubstituted benzoquinones). This occurs since in this case, the outer reorganization term should not be affected as both structures present a similar solvation radius, and therefore any observed difference can be associated to inner reorganization effects.

In this work, a comparative study of the changes in the electrochemical kinetic parameters by the presence of different 2,5 and 2,6 disubstituted benzoquinones (R: Cl, CH_3, $C(CH_3)_3$, Figure 1) in acetonitrile is presented. Substituents are chosen on the basis of comparing simple electron-withdrawing or donating capacity (in the case of CH_3 and Cl as substituents). $C(CH_3)_3$ would in turn indicate any influence by steric components (which would be also regarded as field-inductive effects [7, 8]). The study was performed using cyclic voltammetry to analyze the kinetic behavior of the quinone-semiquinone couple for each studied system. Values of the reorganization energy (λ) were obtained, using a variation of the method presented by Nicholson [17]. The influence of the substituents and chemical structure in the stability of the electrogenerated benzosemiquinone intermediates was evaluated by analyzing the spectral structures obtained by Electron Spin Resonance experiments coupled to the electrochemical generation of species (EC-ESR).

Results and discussion

1. Experimental determination of the reorganization energy (λ)

In order to evaluate the effect of the substituents in terms of the reorganization energy (λ), these data were extracted from
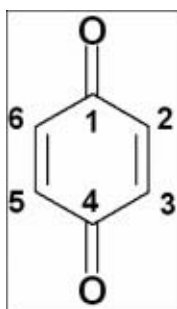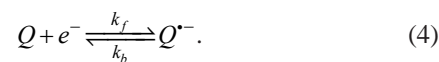

Fig. 1. Structure of the benzoquinone moiety of the molecules studied in this work. Numbers indicate the relative positions of the substituents.

experimental current-potential-time experiments. To achieve this purpose, it is necessary to recognize the kinetic properties of a quasi-reversible electrochemical reduction:

$$Q + e^- \underset{k_b}{\overset{k_f}{\rightleftharpoons}} Q^{\bullet-}. \qquad (4)$$

Q and $Q^{\bullet-}$ represent the quinone and semiquinone species, respectively. For this type of process, the total rate of transformation is controlled by the rate constants of both forward/reduction (k_f) and reverse/oxidation (k_b) processes. The use of transient electrochemical methods to study this type of reactions proves useful. This occurs because the electrochemical response of the product can be also analyzed, even in cases where this species is too unstable to be synthesized. Classically, the apparent rate constant of electron transfer k_s, can be determined employing cyclic voltammetry measurements (Figure 2) using the methodology described by Nicholson [17], by measuring the differences between the cathodic and anodic peak potential (ΔE_{pIc-Ia}) values as a function of the scan rate. However, this case presents a serious disadvantage, as the influence of the transfer coefficient (α) is not apparent, as long as the ΔE_{pIc-Ia} values do not exceed ca. 200 mV [18]. Therefore, in this model it appears as if both k_s and α were independent parameters, as occurs by applying the Butler-Volmer formalism [19, 20] which is not the case (see Introduction).

A more general way of dealing with this problem would be to calculate such variations in terms of λ. For this purpose, a number of values for λ covering the transition between Nernstian and non-Nernstian behavior were chosen (0.7 to 1.4 eV). With these values, k_s can be calculated employing eq. 2, by calculating the pre-exponential factor *A* as the average value of the component of velocity in the direction of the electrode, [10]
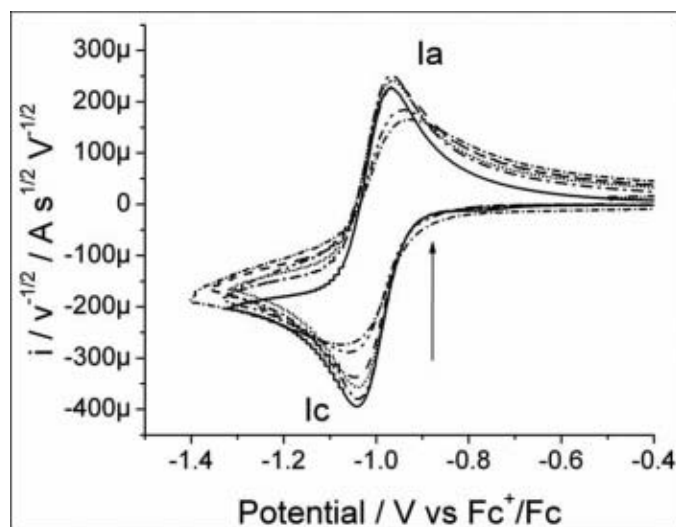

Fig. 2. Cyclic voltammograms obtained for a solution of 0.003 mol L^{-1} 25 MeBQ in 0.1 mol L^{-1} Et_4NBF_4 / CH_3CN, WE: Pt (0.025 cm²), CE: Pt wire. Scan rates shown are 0.03, 0.1, 0.7, 5, 30 and 100 V s⁻¹. Arrow indicates the increase in scan rate. Both the anodic and cathodic signals are indicated.

$$A = (RT/2\pi M)^{1/2}. \qquad (5)$$

It should be noticed that this strategy is a simple way to evaluate the preexponential factor, compared to the pre-equilibrium model which is also used [21]:

$$A = \nu_n K_p \kappa_{el}. \qquad (6)$$

Where K_p is the equilibrium constant of the precursor complex formation process. ν_n is the nuclear frequency factor and κ_{el} is the electronic transmission coefficient. It should be noticed that ν_n is indeed dependent on the activation energy $\Delta G^{\ddagger}$ (or the overpotential $-E - E^0$-, as is presented in electrochemical processes) as follows

$$\nu_n = \tau_L^{-1} \left(\frac{\Delta G^{\ddagger}}{4\pi RT} \right). \qquad (7)$$

This asseveration is only partially correct, as the nuclear frequency factor also depends on the characteristic nuclear frequencies presented by both components (inner and outer) of the reorganization energy [22]

$$\nu_n = \frac{\nu_o^2 \Delta G_o^{\ddagger} + \nu_i^2 \Delta G_i^{\ddagger}}{\Delta G_o^{\ddagger} + \Delta G_i^{\ddagger}}. \qquad (8)$$

Where ν_o and $\Delta G_o^{\ddagger}$ are the characteristic frequency factor and free energy of activation associated to the outer component of the reorganization energy, being the corresponding parameters for the inner reorganization energy designated as ν_i and $\Delta G_i^{\ddagger}$. One interesting aspect commented also by Weaver [22] is that, even when both frequencies (ν_i and ν_o) can exchange their relative magnitudes -since typically ν_i is larger than ν_o-, the final value of this parameter is typically in the order of 1×10^{13} s^{-1}. Furthermore, this value is strongly dependent on the degree of interaction of reactant and product species (particularly the particular vibrational frequencies and free-energy barriers of both), a condition fulfilled usually in homogenous electron transfer rather than in heterogeneous reactions. For a given medium, the longitudinal relaxation time (τ_L) is constant and the consideration that electron transfer occurs in an adiabatic fashion sets the value of k_{el} as -1. Therefore, the corresponding pre-exponential factor (Eq. (6)) is expected to be constant, independently of the variations in the activation energy occurring during the potential scan experiment. Even more, the approach of considering the collisional model to describe the pre-exponential factor (Eq. (5)) has been successfully employed to describe trends in kinetic parameters [23, 24]

Within the chosen approach and for the molecules studied, A have values between 5 to 6 × 10^3 cm s^{-1} (5.5 × 10^3 cm s^{-1} was chosen as a mean value). Both λ and k_s data were inputted in a digital simulation program (Digielch 3.0 ®) to analyze the variations of the ΔE_{pIc-Ia} values from simulated cyclic voltammograms, as a function of the reorganization energy (Figure 3). The experimental data obtained for the compounds presented a fair fit with the calculated curves. The obtained

values for λ for each compound are presented in Table 1. It is important to note that the presented values are not corrected for double layer effects. This occurs because only the trends of kinetic data in terms of the substituent (either by an increase on number, or electron withdrawing or donating capacity), are of interest. For this purpose, D values were also required, and they were evaluated by employing single potential step experiments at potential values where the process is diffusion limited. Then, Cottrell slopes ($i_d*t^{1/2}$ vs t) were determined and from them, mean values (and standard deviations) for D were obtained as suggested by Rosanske and Evans [18] (Table 1). The presented values are quite similar to the ones reported for this type of compounds and were in the order of 2×10^{-5} cm^2 s^{-1}, which was used as the mean value to obtain the working curves shown in Figure 3.
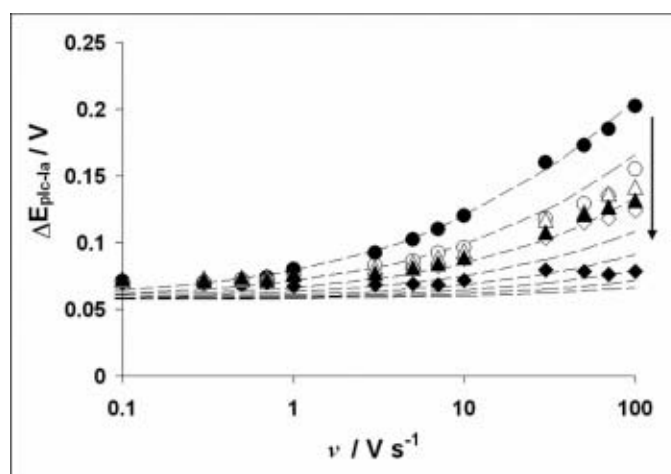

Fig. 3. Variations of the experimental ΔE_{pIc-Ia} values for the studied benzoquinones, as a function of the scan rate: (○) 25MeBQ; (●) 26MeBQ; (◇) 25ClBQ; (◆) 26ClBQ; (Δ) 25tButBQ; (▲) 26tButBQ. Dotted lines depict the calculated ΔE_{pIc-Ia} variations at different reorganization energies: $1.27 > \lambda > 0.94$ eV (D_{model}: 2×10^{-5} cm^2). Arrow indicates decreasing λ values.

Table 1. Calculated formal potentials values ($E^{0'}$), reorganization energies (λ) and diffusion coefficients (D) for the studied benzoquinones.

Quinone	$E^{0'}$ / V vs Fc$^+$/Fc *	D / cm^2 s^{-1} **	λ / eV
25ClBQ	-0.53	2.78 +/- 0.1	1.16 – 1.18
26ClBQ	-0.51	1.51 +/- 0.1	1.02 – 1.08
25MeBQ	-1	2.32 +/- 0.07	1.18 – 1.22
26MeBQ	-1.02	2.14 +/- 0.1	1.26 – 1.28
25tButBQ	-1.05	1.86 +/- 0.05	1.17 – 1.21
26tButBQ	-1.07	2.07 +/- 0.08	1.16 – 1.18

* Obtained as ($E_{pIc} + E_{pIa}$)/2 at 0.1 V s^{-1}.
** Obtained from linear regression of the function $i_d t^{1/2}$ vs t from chronoamperometric experiments [18] (standard deviations from five independent measurements are reported).

The experimental data obtained presented a fair fit with the calculated working curves, being the exception ΔE_{pIc-Ia} from 26ClBQ (Figure 3). However, most of the presented data are comprised between intervals of calculated λ values, and as such are reported in Table 1. It should also be noticed that such deviations occur mostly at the high scan rate region, where the methodology to compensate IR-drop begins to present some failures (even though the employed methodology is considering approximately 95% of the experimental R_u). This could also be a source of error in the data determination, but its extent is not quite large, as most of the obtained data presented a fair fit with the calculated working curves (assuming total compensation).

Nevertheless, the obtained results show that both isomers present different reorganization energies, even though the potential values at which each member of the pair is reduced, is similar. This is indicative of how the chemical properties in the kinetics of electron transfer of the studied compounds are influenced in a particular isomer. Interestingly, for the case of the 2, 5 disubstituted quinones, λ values are very similar regardless of the substituent present (Table 1), on the other hand, 2, 6 disubstitution leads to a sequence in reorganization energies in the trend $Cl < C(CH_3)_3 < CH_3$. This result indicates that simple electron-withdrawing or donating effects are not useful to describe the reactivity sequence observed ($Cl > CH_3 > C(CH_3)_3$ in order of Hammett σ_p values [8]). As commented above, this effect is due to the intrinsic nature of the l values obtained, as they depend on the influence on the substituent on both species participating differing from the case of the standard free Gibbs reaction energy ΔG^0, which normally depends only on the properties of the reacting species [8]. Therefore, it is required to obtain information on the chemical properties of the electrogenerated intermediate to understand the presented kinetic behavior.

2. Relationships between the spectral structure of the electrogenerated substituted benzosemiquinones and the kinetic data

From the above presented analysis, it remains to evaluate how do the chemical properties of the electrogenerated semiquinone are influenced by the reorganization processes. This can be useful to evaluate both the final destination of the electron density added to the quinone moiety and the lability of the radical species generated. For this purpose, coupled Electrochemical-Electron Spin Resonance (EC-ESR) experiments were carried out to obtain ESR spectra of the electrogenerated species. In the case of chlorine substituted compounds the ESR spectra of the corresponding semiquinones is presented in Figure 4.

It is noticeable the characteristic spectrum of 25ClBQ (Figure 4A), as it lacks of a proper structure that could be assigned to a single radical species generated. This spectrum can be originated by a mixture of radical species generating in the electrolysis cell. This result implies that the electron transfer process is coupled to a follow-up chemical reaction which consumes the radical species and generates another
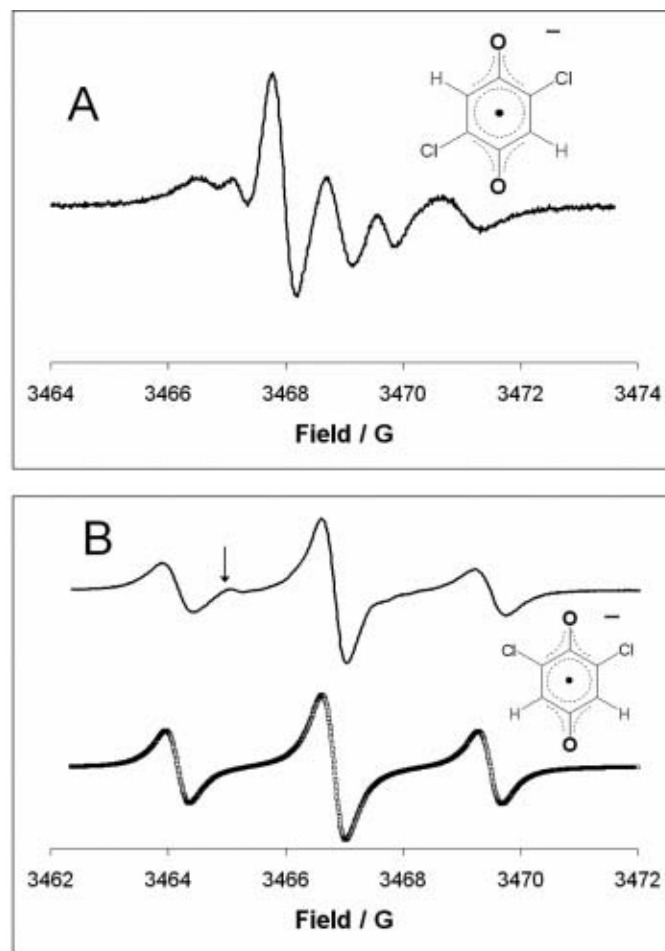

Fig. 4. ESR spectra for the electrogenerated semiquinone of (A) 1 mM 25ClBQ and (B) 26ClBQ in 0.1 M Et_4NBF_4 / CH_3CN. Modulation amplitude: 0.01 G. Solid lines indicate the experimental spectrum, while points indicate simulated spectra from calculated HFCC. Arrow indicates the presence of another signal in the 26ClBQ semiquinone spectrum.

radical structure as a result. The rate constant of this process are not expected to be high enough, since in results previously considered in the literature, no mentions for its existence are stated [16]. However, under the thin layer electrolysis condition of the cell (cell width of nearly 0.5 mm), the speed of the process would be in the second scale, and so it was possible to detect it at the higher time scale of the EC-ESR measurements. 26ClBQ behaves in a most different way (Figure 4B), since the main triplet structure obtained ($a_H = 2.66$ G, Table 2), is consistent with coupling of the unpaired electron with the α-H atoms present in the chemical structure of the corresponding quinone. However, a small signal is appearing at fields of nearly the same g value of the analyzed compound (at nearly 3465 G or about 2.0035 vs 2.0047 of 26ClBQ, Figure 4B). This indicates that, as in the case of 25ClBQ, the electrogenerated semiquinone presents a coupled chemical process after the electron transfer. However, the rate constant of this process

Table 2. Experimental Hyperfine Coupling Constants (HFCC), linewidths (Γ) and g values obtained from ESR spectra of the electrogenerated semiquinone species for the studied benzoquinones

Quinone	a_3 / G	a_5 / G	a_6 / G	aCH_3 / G	Γ / G	g
25ClBQ	ND	NA	ND	NA	0.42	ND
	(2.24)		(2.24)			
26ClBQ	2.66	2.66	NA	NA	0.34	2.0047
	(2.55)	(2.55)				2.0035*
25MeBQ	1.97	NA	1.97	2.16	0.07	2.0051
	(2.06)		(2.06)	(1.94)		
26MeBQ	2.21	2.21	NA	1.85	0.19	2.0043
	(2.40)	(2.40)		(1.67)		
25tButBQ	2.23	NA	2.23	NA	0.17	2.0049
	(2.46)		(2.46)			
26tButBQ	2.03	2.03	NA	NA	0.18	2.0045
	(2.84)	(2.84)				

NA: Not applicable as the position is bearing another substituent; ND: Not determined.
* Data for the second radical structure observedValues in parenthesis indicate calculated HFCC using the B3LYP/3-21G(d,p) method.

is not the same as in 25ClBQ, since most of the detected radical species arises from the 26ClBQ semiquinone.

Considering the low energy of reorganization obtained for this pair of isomers (Table 1), the reaction occurring after the electron transfer process is proposed to be a follow-up chemical cleavage [25] of the halogen atom after the electroreduction of the semiquinone. In general terms, the undergoing chemical pathway can be represented by the next set of chemical equations, where QX is the halogen (X) substituted benzoquinone:

$$QX + e^- \rightleftharpoons QX^{\bullet -} \qquad (9)$$

$$QX^{\bullet -} \rightarrow Q^{\bullet} + X^-. \qquad (10)$$

This effect occurs for the experimental cases on the time scale reported for CH_3CN solution [26], and shows that for both chlorine substituted quinones, Eq. (10) is the rate determining step. Interestingly, the stability of the electrogenerated $QX^{\bullet -}$ is a function of the chemical structure of the compound, being the 2, 5 disubstituted radical less stable compared to the 2, 6 disubstitution, which could be related to the higher reorganization energy in the former compound than in the latter. The higher λ value of the pair (for 25ClBQ, Table 1) could account for the dissociation energy related to eq. 7 [27].

Methyl-substituted benzoquinones 25MeBQ and 26MeBQ were also studied using this methodology. These compounds, as in the case of Cl substituted quinones, prove to be thermodynamically non-differentiable, as their experimental $E^{0'}$ values are nearly the same (Table 1). The obtained ESR spectra of these compounds are presented in Figures 5A and 5B.

Both quinone compounds differ in the value for the hyperfine coupling constants for the H atoms in the quinone ring and those present in the methyl group (Table 2). As a fact of importance, both sets of values seem to be inverted for each
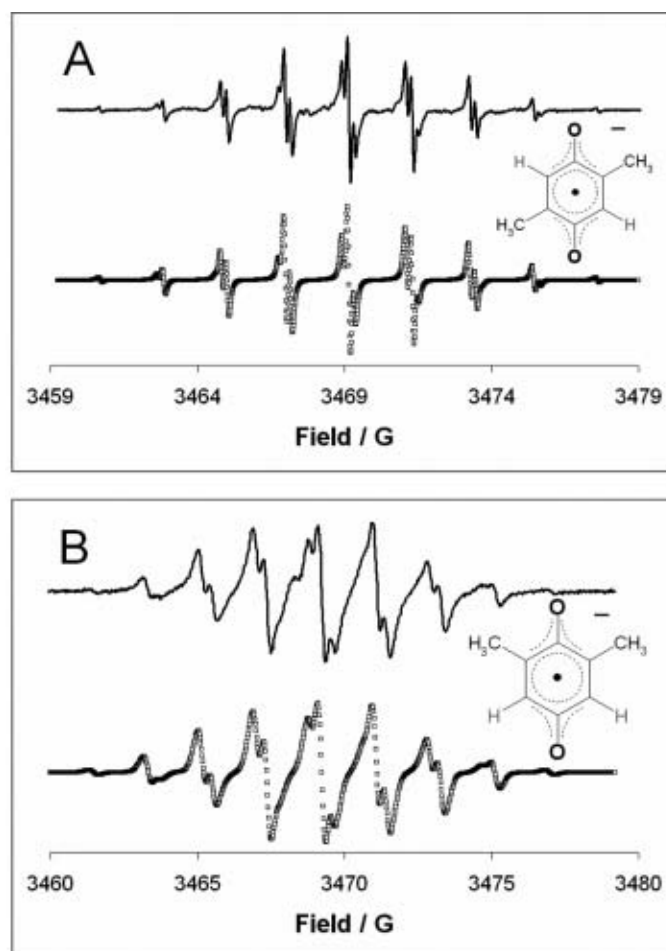

Fig. 5. ESR spectra for the electrogenerated semiquinone of (A) 1 mM 25MeBQ and (B) 26MeBQ in 0.1 M Et_4NBF_4 / CH_3CN. Modulation amplitude: 0.01 G. Solid lines indicate the experimental spectrum, while points indicate simulated spectra from calculated HFCC.

compound. It is important to recall that HFCC values are an experimental estimate of the spin density ρ according to the McConnell equation [28]

$$a = Q\rho. \qquad (11)$$

On this basis, the behavior of 25MeBQ and 26MeBQ shows that the spin density sites change due to the relative position of the methyl substituent. Moreover, the experimental linewidth is different for both semiquinone compounds (Table 2). This is important, as linewidth (Γ) data are related to the self-exchange electron transfer kinetics in solution between the electrogenerated radicals and the neutral species remaining in solution [38]. From this data, the inner reorganization energy shows to be lower for the 26MeBQ than for 25MeBQ, as the former has a lower Γ value.

An estimate of the inner reorganization energy can be calculated, as this quantity would contain the information regarding only nuclear reorganization (and not solvent components) occurring in the Q → Q$^{\bullet-}$ transformation, as it would be useful to consider the kinetic differences presented by both isomers. A rather simple approach to estimate the λ_i term has been presented earlier by Nelsen [29], where the inner reorganization energy can be estimated from the difference in energy of the electron self-exchange reaction ($\lambda_{i,\,exch}$),

$$Q + Q^{\bullet-} \rightarrow Q^{\bullet-} + Q. \qquad (12)$$

This is possible as, in this type of reactions, the nuclear configurations of the reactant and products are adjusted to be the same without effectively transferring the electron. Therefore, the inner reorganization energy for the self-exchange reaction (Eq. (12)), can be estimated by:

$$\lambda_{i,exch} = [E(N\,as\,RA) - E(N\,as\,N)] + [E(RA\,as\,N) - E(RA\,as\,RA)] \quad (13)$$

Where E(X as Y) represents the energy of the species X within the optimized molecular structure of species Y. The two species participating during the electron transfer process are the neutral quinone (N) and the semiquinone (RA). For this purpose, these calculations can be performed employing single point procedures for the optimized structures of N and RA for each quinone compound. In the case of a heterogeneous electron transfer process with only one reactant participating, the inner reorganization energy would be half the value calculated in eq. 10. However, the calculated values with this procedure employing the B3LYP/3-21G(d,p) for both compounds are very similar (0.19 eV), and do not allow to compare the effects observed experimentally. Moreover, outer reorganization effects are not expected to be significantly different between both compounds, as the calculated diffusion coefficients are very similar (Table 1), and therefore the solvation radius would be the same for each. Therefore, the observed differences could be related to the changes in the spin density distribution for each quinone. This is relevant, as the model of Marcus-Hush employed for the analysis relies on the estimation of the

reorganization energies as global parameters, rather than in local properties of the participating species. This factor could be important for improving the dynamic theoretical description of this type of systems.

In the case of benzoquinones disubstituted with C(CH$_3$)$_3$ groups (25tButBQ y 26tButBQ), the ESR spectra for the corresponding electrogenerated semiquinones are presented in Figure 6.

From the analysis of the HFCC between the electron spin and the H atoms in the quinone ring, a similar behavior as presented by the methyl derivatives was obtained: HFCC values associated with a protons show differences in terms of the isomer which bears the C(CH$_3$)$_3$ groups. The obtained data show that the highest spin density resides at the C-3 and C-6 positions for the case of the 2, 5 isomer. Meanwhile, for the 2, 6-disubstituted quinone, most of the spin density resides in the positions bearing the C(CH$_3$)$_3$ groups. However, these differences are lower in value compared to the case of methyl substituted quinones, which would account for the slight difference in reorganization energies. This could be due to the
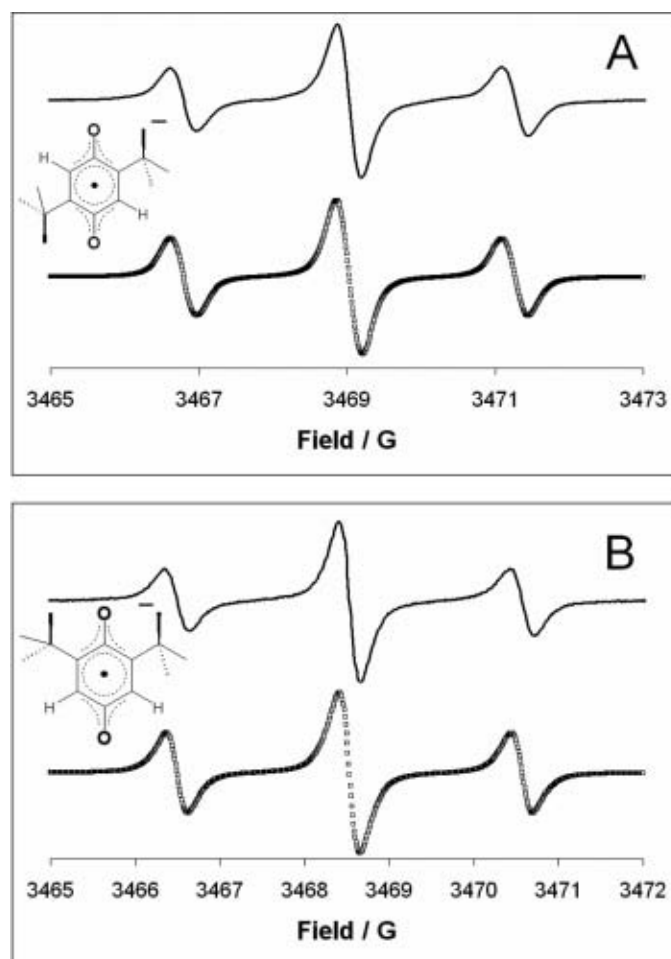

Fig. 6. ESR spectra for the electrogenerated semiquinone of (A) 1 mM 25tButBQ and (B) 26tButBQ in 0.1 M Et$_4$NBF$_4$ / CH$_3$CN. Modulation amplitude: 0.01 G. Solid lines indicate the experimental spectrum, while points indicate simulated spectra from calculated HFCC.

bulky nature of the $C(CH_3)_3$ substituent, which makes electronic inductive effects less pronounced as in the other cases. The calculation of the inner reorganization component by the B3LYP/3-21G(d,p) showed that 25tButBQ has a lower λ_i value (0.19 eV), compared to 26tButBQ (0.24 eV), which is opposed as the experimental tendency in total λ values (Table 1). Therefore, the remaining reorganization energy is strongly affected by solvation dynamics, which would complement the inner reorganization component.

Conclusions

The effect of 2,5 and 2,6 disubstitution (R = CH_3, Cl, $C(CH_3)_3$) for 1,4-benzoquinones, in the reorganization energy (λ) for the first electron uptake process was analyzed in acetonitrile solution. Data obtained by cyclic voltammetry suggested differences in λ for each type of disubstitution analyzed. Considering that the compared molecules have similar radius, the observed differences can be understood considering changes in the inner component of λ. These differences have important consequences in the stability and structure of the electro-generated benzosemiquinone species, as proved for Cl substituted 1,4-benzoquinones, where a chemical cleavage of the C-Cl bond occurs after the first electron uptake, being the rate constant of this process determined by the particular structure of the studied disubstituted compound. This fact was verified by performing *in situ* spectroelectrochemical-ESR (Electron Spin Resonance) experiments of each disubstituted semiquinone. These experiments were also useful to describe the differences in λ for the CH_3 and $C(CH_3)_3$ substituted benzoquinones, in terms of spin exchange processes and distribution of the spin density, respectively.

Experimental

Substances

2, 5-dimethyl-1,4-benzoquinone [25MeBQ], 2, 6-dimethyl-1,4-benzoquinone [26MeBQ], 2, 5-dichloro-1,4-benzoquinone [25ClBQ], 2, 6-dichloro-1,4-benzoquinone [26ClBQ], 2, 5-ditertbutyl-1,4-benzoquinone [25tButBQ] and 2, 6-ditertbutyl-1,4-benzoquinone [26tButBQ]. Benzoquinones were resublimed prior to their use. All the substances were obtained from Aldrich ® except 25MeBQ which was obtained from Fluka Chemika ®.

Solvent and Supporting Electrolyte

Anhydrous Acetonitrile (CH_3CN, Aldrich 98%) was dried overnight with P_2O_5 and distilled prior to use. The distillate was received over oven-activated 3 Å molecular sieves (Merck) and kept in a desiccator. The method is useful to obtain dry acetonitrile, characterized by the absence of OH bands in IR spectra. Tetraethylammonium tetrafluoroborate (Fluka Chemika, Electrochemical grade, Et_4NBF_4) was used as a supporting electrolyte. The salt was dried the night before use at 90°C and 0.1 mol L^{-1} solutions were prepared and used as the supporting electrolyte.

Electrochemical determinations

Cyclic voltammetry at several scan rates within the interval: $0.01 = v = 100$ Vs^{-1}, and chronoamperometry experiments were performed, applying IR drop compensation with R_u values determined from positive feedback measurements (R_u: 142 Ohms). [30, 31], in an AUTOLAB PGSTAT 100 potentiostat/galvanostat. A conventional three electrode cell was used to carry out these experiments, employing as the working electrode a platinum microelectrode (BAS, Surface: 0.025 cm^2), polished using 0.05 μm alumina (Büehler), sonicated in distilled water for 10 minutes and rinsed with acetone prior to use. The polishing process was performed after the electrochemical study of each compound. Between each voltammetric and chronoamperometric run for the electrochemical study of each compound, the electrode was rinsed with acetone. These procedures allowed good reproducibility in the experimental results. A platinum mesh was used as the counterelectrode (Surface: 0.6 cm^2).The potential values were obtained against the reference (Bioanalytical Systems, BAS) of Ag/0.01 mol L^{-1} $AgNO_3$ + 0.1M Tetrabutylammonium perchlorate (Bu_4NClO_4) in acetonitrile, separated from the medium by a Vycor membrane. Potential values are reported versus the ferricinium/ferrocene couple (Fc^+/Fc), according to the IUPAC recommendation [32]. The potential of the Fc^+/Fc couple was measured for each separate compound in order to avoid changes in potential due to modifications of the reference potential caused by the Vycor aging.

Electrochemical experiments were carried out as follows: 0.003 mol L^{-1} solutions of the studied quinones were prepared by dissolving the proper sample in 0.1 mol L^{-1} tetraethylammonium tetrafluoroborate (Et_4NBF_4) in acetonitrile (CH_3CN) solution. With these prepared solutions, both cyclic voltammetry was performed in the scan rate range from 0.01 to 100 Vs^{-1}. All the obtained potentials are referred to the Fc^+/Fc couple as recommended by the IUPAC [32].

EC-ESR Spectroscopy Experiments

ESR spectra were recorded in the X band (9.85 GHz) using a Brucker ELEXSYS 500 instrument with a rectangular TE011 cavity. A commercially available spectroelectrochemical cell (Wilmad) was used, employing as the working electrode a 0.02 mm platinum wire (3.1 cm^2), introduced in the flat path of the cell. Another platinum wire was used as counter electrode (2.5 cm^2). The reference of Ag/0.01 mol L^{-1} $AgNO_3$ + 0.1M Bu_4NClO_4 in acetonitrile (BAS) was employed as the reference electrode. Potential sweep control was performed with a 100 B/W Voltammetric Analyzer of Bioanalytical Systems (BAS) interfaced with a personal computer. Solutions of quinones for these experiments were prepared by dissolving the

desired compound in 0.1 mol L^{-1} Et$_4$NBF$_4$ to reach a 0.001 mol L^{-1} concentration. The solutions were deoxygenated for 30 minutes and the cell was kept under a nitrogen atmosphere (grade 5, Praxair) throughout the experiment.

ESR simulations

PEST WinSim free software Version 0.96 (National Institute of Environmental Health Sciences) was used to perform simulation of the ESR experimental spectra, from the measured hyperfine coupling constant values (HFCC). This program was also useful to evaluate HFCC values when a direct measurement would be difficult in the conditions where the spectra acquisition was performed.

Theoretical calculations

PM3 calculations [33, 34, 35] were performed with HyperChem (HyperCube Inc.) Ver. 7.51 to perform full geometry optimization (no geometry constrains) for the radical structures experimentally detected, employing UHF (Unrestricted Hartree-Fock) calculations. Vibrational analysis was performed to check that the obtained structures were indeed the minimum energy conformers, characterized by the lack of negative vibrational frequencies. These structures were used as inputs for single point energy calculations. Single point energy calculations were performed with the 3-21G(d,p) basis set [36] using the hybrid functional of Becke and Lee-Yang-Parr (B3LYP) [37] to account for electron correlation. From this data, spin densities values were evaluated as the difference between α and β spin densities (From s type orbitals in the case of H atoms), multiplied by the corresponding Hyperfine Coupling Constant between the involved atom and the unpaired electron in the gas phase (506.9 Gauss for H atoms [38])

Acknowledgments

References

1. Bolton, J.L.; Trush, M.A.; Penning, T. M.; Dryhurst, G.; Monks, T. J. *Chem. Res. Toxicol.* **2000**, *13*, 135-160
2. Brunmark, A.; Cadenas, E. *Free Rad. Biol. Med.* **1989**, *7*, 435-477
3. Ksenzhek, O. S.; Petrova, S. A.; Kolodyazhny, M. V.; Oleinik, S. V. *Bioelectrochem. Bioenerg.*, **1977**, *4*, 335-345
4. González, F. J.; Aceves, J. M.; Miranda, R.; González I. *J. Electroanal. Chem.* **1991**, *310*, 293-303
5. Aguilar-Martínez, M.; Bautista-Martínez, J.A.; Macías-Ruvalcaba, N. A.; González, I.; Tovar, E.; Marín del Alizal, T.; Collera, O.; Cuevas, G. *J. Org. Chem.* **2001**, *66*, 8349-8363
6. Ferraz, P. A. L.; Abreu, F. C.; Pinto, A. V.; Glezer, V.; Tonholo, J.; Goulart, M. O. F. *J. Electroanal. Chem.* **2001**, *507*, 275-286
7. Zuman, P. *Collection Czech. Chem. Commun.* **1960**, *25*, 3225-3244
8. Èársky, P.; Zuman, P. *Collection Czech. Chem. Commun.* **1969**, *34*, 497-503
9. Janzen, E. G. *Acc. Chem. Res.* **1969**, *2*, 279-288
10. Marcus, R. A. *J. Chem. Phys.* **1956**, *24*, 966-978
11. Marcus, R. A. *Electrochim. Acta*, **1968**, *13*, 995-1004
12. Hush, N. S. *J. Chem. Phys.*, **1958**, *28*, 962-972
13. Hush, N. S. *Electrochim. Acta* **1968**, *13*, 1005-1023
14. Bard, A. J.; Faulkner, L. R. *Electrochemical methods. Principles and applications*. 2nd edition. John Wiley and Sons, United States of America. **2001**
15. Rüssel, Ch.; Jaenicke, W. *Z. Phys. Chem. N. F.* **1984**, *139*, 97-112
16. Clegg, A. D.; Rees, N. V.; Klymenko, O. V.; Coles, B. A.; Compton, R. G. *J. Phys. Chem. B.* **2004**, *108*, 13047-13051
17. Nicholson, R. S. *Anal. Chem.* **1965**, *37*, 1351-1355
18. Rosanske, T. W.; Evans, D. H. *J. Electroanal. Chem.* **1976**, *72*, 277-285
19. Butler, J. A. V. *Trans. Faraday. Soc.*, **1924**, *19*, 729-733 and 734-739
20. Erdey-Grúz, T.; Volmer, M. *Z. Phys. Chem.* **1930**, 150A, 203-213
21. Weaver, M. J. *Redox Reactions at Metal-Solution Interfaces* (Chapter 1) in *Comprehensive Chemical Kinetics*, R. G. Compton (ed); Volume 27: **Electrode Kinetics: Reactions**, Elsevier Science and Technology, 1987
22. Hupp, J. T.; Liu, H. Y.; Farmer, J. K.; Gennett, T.; Weaver, M. J. *J. Electroanal. Chem.* **1984**, *168*, 313-334
23. Rüssel, Ch.; Jaenicke, W. *J. Electroanal. Chem.* **1986**, *200*, 249-260
24. Saveant, J. M.; Tessier, D. *J. Phys. Chem.* **1977**, *81*, 2192-2197
25. Andrieux, C. P.; Hapiot, P.; Savéant, J. M. *J. Phys. Chem.* **1988**, *92*, 5987-5992
26. Wipf, D. O.; Wightman, R. M. *J. Phys. Chem.* **1989**, *93*, 4286-4291
27. Savéant, J. M. *Elements of Molecular and Biomolecular Electrochemistry*. Wiley Interscience. New Jersey, Chapter 3. **2006**
28. McConnell, *J. Chem. Phys.*, **1956**, *24*, 764
29. Nelsen, S. F.; Blackstock, S. C.; Kim, Y. *J. Am. Chem. Soc.* **1987**, *109*, 677-682
30. Roe, D. K. "*Overcoming Solution Resistance with Stability and Grace in Potentiostatic Circuits*" in *Laboratory Techniques in Electroanalytical Chemistry*, Kissinger, P. T. and Heineman, W. R. (Editors). Marcel Dekker, Inc. New York, USA. **1996**
31. He, P.; Faulkner, L. R. *Anal. Chem.* **1986**, *58*, 517-523
32. Gritzner, G.; Küta, J. *Pure Appl. Chem.*, **1984**, *4*, 462
33. Stewart, J. P. P. *J. Comput. Chem.* **1989**, *10*, 209 and 221
34. Stewart, J. P. P. *J. Comput. Chem.* **1990***, 11*, 543
35. Stewart, J. P. P. *J. Comput. Chem.* **1990**, *12*, 320
36. Pietro, W. J.; Francl, M. M.; Hehre, W. J.; Defrees, D. J.; Pople, J. A.; Binkley, J. S. *J. Am. Chem. Soc.* **1982***, 104*, 5039-5048
37. Becke, A. D. *J. Chem. Phys.* **1993***, 98*, 5648
38. Wertz, J. E.; Bolton, J. R. *Electron Spin Resonance*. First edition, Chapman and Hall, New York, **1972**